

Neutral pion production in the $^{16}\text{O} + ^{27}\text{Al}$ reaction at 94 MeV/nucleon

A. Badalá,⁽¹⁾ R. Barbera,⁽¹⁾ A. Palmeri,⁽¹⁾ G. S. Pappalardo,⁽¹⁾ F. Riggi,^(1,2) A. C. Russo,^(1,2)
 C. Agodi,⁽³⁾ R. Alba,⁽³⁾ G. Bellia,^(2,3) R. Coniglione,⁽³⁾ A. Del Zoppo,⁽³⁾ P. Finocchiaro,⁽³⁾ C. Maiolino,⁽³⁾
 E. Migneco,^(2,3) P. Piattelli,⁽³⁾ G. Russo,^(2,3) P. Sapienza,⁽³⁾ and A. Peghaire⁽⁴⁾

⁽¹⁾*Istituto Nazionale di Fisica Nucleare, Sezione di Catania, Corso Italia 57, I95129 Catania, Italy*

⁽²⁾*Dipartimento di Fisica, Università di Catania, Corso Italia 57, I95129 Catania, Italy*

⁽³⁾*Istituto Nazionale di Fisica Nucleare, Laboratorio Nazionale del Sud, Catania, Italy*

⁽⁴⁾*Grand Accélérateur National d'Ions Lourds, Caen, France*

(Received 3 December 1991)

The production of neutral pions in the reaction $^{16}\text{O} + ^{27}\text{Al}$ at 94 MeV/nucleon was studied with a multidetector, which includes 180 BaF₂ modules. Kinetic energy spectra for several laboratory angles were measured. The total cross section for neutral pion production was deduced. Results were compared with previous findings on charged pions from the same reaction at the same energy and with the prediction of a dynamical model based on the numerical solution of the Boltzmann-Nordheim-Vlasov equation.

PACS number(s): 25.70.-z

I. INTRODUCTION

Production of charged as well as neutral pions has been studied over the past years at energies significantly lower than the absolute free nucleon-nucleon ($N-N$) threshold [1]. The relatively large cross sections observed in nucleus-nucleus collisions at energies as low as 25 MeV/nucleon have been understood in terms of the Fermi momentum which couples to the relative motion of the colliding nuclei and/or of cooperative effects involving several nucleons from the projectile and target. Semi exclusive experiments on charged pion production have been carried out around 100 MeV/nucleon [2,3] with the aim of looking at the velocity and angular distributions of the associated light charged particles and, hence, to get information on the violence of the collision.

In case of neutral pions, some of the experimental limitations which are inherent to charged pions can be overcome: (i) A large solid angle can be covered employing a large array of γ detectors; (ii) energy spectra can be measured down to very low kinetic energies, where the maximum cross section is usually found in this energy domain. Moreover, pion reabsorption and any final-state interaction between the emitted pions and residual nuclear matter can be easily disentangled from Coulomb effects.

Along this line a few inclusive experiments on neutral pion production at energies 25–100 MeV/nucleon have been reported [4–8]. Most of these experiments have been carried out by lead glass Cherenkov counters to detect the two γ rays originating from the π^0 decay. A recent review [9] has discussed the various techniques employed in the earlier experiments. Only recently has the availability of large-volume BaF₂ scintillation detectors allowed the exploitation of the interesting discriminating features of this scintillator material for the detection of hard photons and light charged particles, and arrays of such scintillators have been built for exclusive

measurements in heavy-ion reactions at intermediate energies [10–13].

The use of these large arrays of detectors will allow for exclusive measurements of pion production, in which a large part of the reaction products will be detected in coincidence with a pion trigger, thus giving, in principle, the possibility to measure global variables which give an overall description of the event and to extract the impact parameter for the collisions producing pions [14].

In view of future exclusive experiments with this new experimental setup, a preliminary inclusive experiment was undertaken with the detector MEDEA (multielement detector array) [12], on the reaction $^{16}\text{O} + ^{27}\text{Al}$ at 94 MeV/nucleon, in order to compare neutral and charged pion production at the same energy and on the same system [2,3,15]. An additional motivation for this study was to compare the information extracted from BaF₂ arrays to that obtained with lead glasses.

II. EXPERIMENT AND DATA ANALYSIS

The experiment was carried out at GANIL, by using an ^{16}O beam at 94 MeV/nucleon. A 1.6-mg/cm²-thick ^{27}Al target was bombarded with an average beam current of a few nA. The pulsed beam had a 0.6-ns width, while the repetition rate was 13.3 MHz.

Figure 1 gives a sketch of the experimental setup. Neutral pions were detected through their main (98.8%) decay branch into two γ rays. The BaF₂ modules of MEDEA multidetector were used. They are arranged into eight annular rings, covering the polar angles from 30° to 170°. Each ring is segmented into 24 detectors, each spanning $\Delta\varphi = 15^\circ$ except for the last backward ring, which only includes 12 detectors. In the present experiment, one ring was missing at backward angles, thus reducing the number of BaF₂ modules to 180. Each BaF₂ module has a tapered shape with a trapezoidal cross section with a length of 20 cm, and it is placed 22 cm from

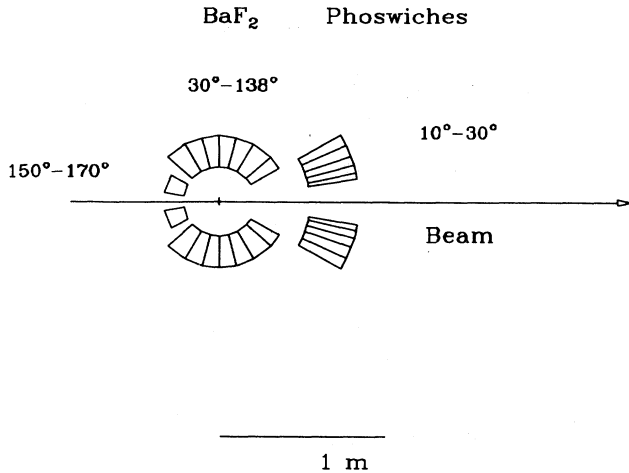


FIG. 1. Sketch of the experimental setup. The set of BaF₂ modules is shown together with the phoswich detectors at forward angles. In the present experiment, the trigger was generated by any twofold coincidence of the six BaF₂ rings around 90°.

the target. The MEDEA array also includes a set of 120 phoswich detectors, arranged into five rings of 24 detectors each and covering polar angles from 10° to 30°. The whole system operates in a vacuum vessel at pressures around 10^{-6} mbar. A complete description of the detector, together with its properties, is reported elsewhere [12]. For this experiment the trigger was generated by any twofold coincidence of the BaF₂ modules belonging to the six rings around $\vartheta=90^\circ$. A threshold roughly corresponding to 18 MeV γ -equivalent energy was imposed for each detector on the trigger logic. Photon-hadron separation was achieved by time-of-flight and pulse-shape analyses employing the fast and total components of the light output from the BaF₂ scintillators. Calibration of the detectors was determined both with γ rays from radioactive sources and by the response of the detectors to cosmic rays. The reconstruction of the incident photon energy is not a trivial problem since the electromagnetic shower initiated by hard photons in a given detector usually develops in the neighboring ones. The improvement in the photon energy reconstruction, which can be obtained by summing up the energy deposited in all the detectors interested by the shower, was carefully studied in order to define the granularity and crystal size of the MEDEA array [12]. The response of BaF₂ detectors of similar size (20 cm long, 5.2 cm inner diameter, hexagonal shape) to photons of 3–50 MeV energy has been recently reported [16], and it was shown that the experimental spectra can be well reproduced by electromagnetic shower simulations with the Monte Carlo code GEANT3 [17]. For the experiment presented here, further calculations [18] were carried out with the code GEANT3 with the purpose to study the overall response of the array to neutral pions decaying into two gamma rays.

The information associated with the different involved detectors allows one to extract more reliable values of the energy and emission angle of the two photons originating from the pion decay. In this experiment several of the BaF₂ modules were not active, this fact being taken into

account to extract from the simulations a reliable efficiency. Because of the limited statistics, however, it was not possible for this preliminary experiment to consider only those events for which the two electromagnetic showers are fully reconstructed (both clusters of detectors considered). To extract the invariant mass and energy spectra, the analysis was thus extended to those events involving two counters which have at least one cluster of detectors around them.

Since no laser-based monitoring system is yet in operation for the multidetector MEDEA, possible shifts or drifts of the gain during the experiment can be expected, as for similar detectors [13]. This was accounted for by comparing the energy spectra for all detectors in each run (30 min long) to the corresponding spectra of a reference run and correcting the calibration of each run whenever required.

Figure 2 shows the experimental invariant mass distribution obtained from the reaction $^{16}\text{O}+^{27}\text{Al}$ at 94 MeV/nucleon. This was obtained after proper discrimination of the gammas against the hadrons in the fast total and energy time-of-flight matrices. For further background suppression, only events with relative angles between the two showers, $\vartheta_{12} > 90^\circ$, were considered. From simulation it was estimated that this cut introduces no yield loss for pions with kinetic energy lower than 40 MeV and about 7% at 50 MeV. The loss increases with the kinetic energy of the pions, but it was verified that the overall effect on the efficiency correction amounts to a few percent of the total yield, since the cross section is mainly dominated by low-energy pions. Moreover, the condition $E_1 + E_2 > 100$ MeV (E_1 and E_2 being the energies of the two showers) was also imposed in order to exclude possible events in which the showers are badly reconstructed as a result of the large energy leakage.

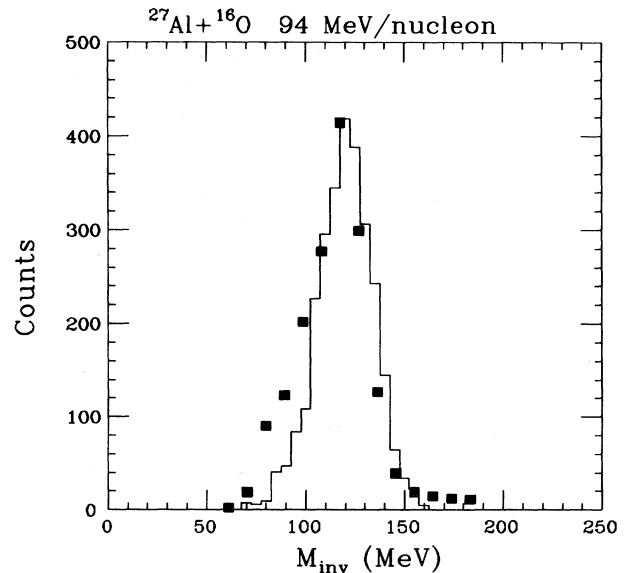


FIG. 2. Invariant mass spectrum from the $^{16}\text{O}+^{27}\text{Al}$ reaction at 94 MeV/nucleon. The peak around 120 MeV corresponds to neutral pions. The spectrum is compared to the result of a GEANT3 calculation (solid histogram).

The angles of the two detected gammas were extracted by a weighted mean over the energy deposited in each detector of the cluster. Using energy and linear momentum conservation, it is possible to evaluate the energy and emission angle of the neutral pion from the measured energies and angles of the two decay photons. When the γ -ray energy resolution is not so good, it is usual to extract the π^0 total energy from [19,20]

$$E_{\pi^0}^2 = \frac{2m_0^2}{(1 - \cos\vartheta_{12})(1 - X^2)}, \quad (1)$$

where m_0 is the π^0 rest mass, ϑ_{12} is the relative angle between the two showers, and the asymmetry parameter X is defined by

$$X = \frac{E_1 - E_2}{E_1 + E_2}, \quad (2)$$

E_1 and E_2 being the energies of the two showers.

Relative merits of this method of analysis, which is less sensitive to uncertainties in the energies E_1 and E_2 , have been discussed in Refs. [19,20]. With this choice the invariant mass is given by

$$m = 2\sqrt{E_1 E_2} \sin(\vartheta_{12}/2) \quad (3)$$

and the kinetic energy T_{π^0} is obtained by $T_{\pi^0} = E_{\pi^0} - m_0$. The emission angle ϑ_{π^0} of the pion is extracted by

$$\cos\vartheta_{\pi^0} = \frac{P_{\parallel}}{P_{\text{tot}}} = \frac{E_1 \cos\vartheta_1 + E_2 \cos\vartheta_2}{(E_1^2 + E_2^2 + E_1 E_2 \cos\vartheta_{12})^{1/2}}. \quad (4)$$

The results of these GEANT3 simulations are fully reported in Ref. [18]. In that work it was shown that for low-energy pions the efficiency of the full array is very close to the geometrical limit, whereas for higher kinetic energies the efficiency decreases at forward and backward directions, being almost constant near 90° . It was also shown that a realistic kinetic energy spectrum is correctly reconstructed by this procedure, which was adopted also for the present data, thus allowing one to measure the slope parameters.

Under these conditions a peak in the invariant mass spectrum is seen at 120 MeV, with a full width at half maximum around 30 MeV. The solid histogram is the result of a GEANT3 simulation carried out using realistic energy and angular distributions of the emitted pions and including the effects of the geometry, collection efficiency, and cuts on the experimental data. Also, differences in the energy thresholds for each detector due to different calibration parameters and offsets were introduced in the simulation. The effect of fluctuations in the gain of the single modules, not totally corrected by the procedure described before, was also introduced in the simulation by a Gaussian spreading around the nominal value. The lack of several BaF_2 modules reduces the efficiency with respect to that which is obtained by the use of the full array, as reported in Ref. [18]. A reasonable agreement of the invariant mass spectrum is found with the simulation, suggesting that most of the experimental effects are properly taken into account in the efficiency evaluation. To

extract energy spectra at different laboratory angles from the data, a cut was imposed on the invariant mass spectrum between 50 and 160 MeV.

III. EXPERIMENTAL RESULTS AND DISCUSSION

Figure 3 shows the invariant cross section $(1/p)d^2\sigma/d\Omega dT_{\pi^0}$ of neutral pions for different regions of the pion emission angle. All spectra were corrected for the experimental efficiency, calculated by including the effects already discussed. A fit of these spectra carried out on the exponential tail through $\exp(-T_{\pi^0}/E_0^{\text{inv}})$ gave the values of the inverse slope parameter E_0^{inv} reported in Table I.

Experimental values of the inverse slope parameter for charged and neutral pions as a function of the incident energy have been discussed by several authors [1]. However, the data reported so far are not easily comparable, since these parameters have been extracted by using both laboratory energy spectra and/or invariant cross sections which have been fitted by an exponential falloff. Moreover, some authors report the values obtained from the angle-integrated cross section, while some dependence on the emission angle is usually found. The energy range used to fit the data to an exponential shape can also influence the obtained results. For this reason a detailed comparison of the results could be of interest, provided that they are treated in a consistent way. For sake of completeness, inverse slope parameters E_0^{lab} were also extracted from the laboratory energy spectra shown in Fig. 4. Table I reports the values of the slope parameter obtained from the present investigation, together with the results obtained for charged pions at the same incident energy.

An angle dependence of the slope parameter is ob-

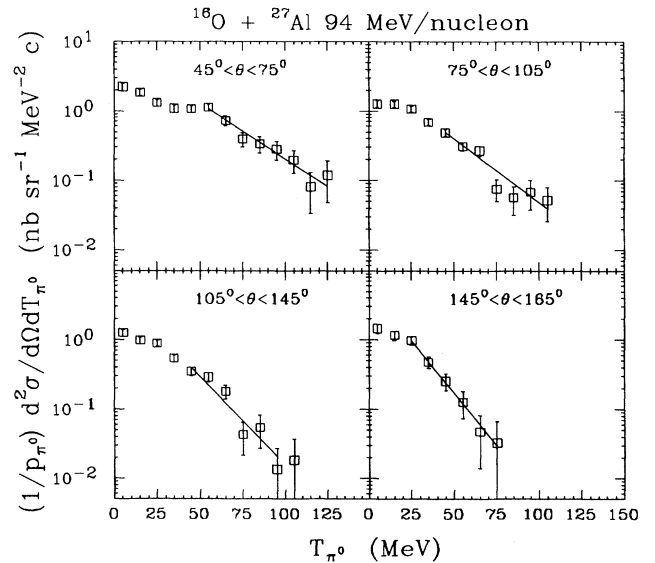


FIG. 3. Invariant cross sections for the production of neutral pions from the $^{16}\text{O} + ^{27}\text{Al}$ reaction at 94 MeV/nucleon. Solid lines are the result of a fit on the exponential tail to extract the slope parameter reported in Table I (see text).

TABLE I. Inverse slope parameters used to fit laboratory energy spectra E_0^{lab} and invariant cross sections E_0^{inv} from experiments on charged and neutral pion production.

System	Energy (MeV/nucleon)	ϑ_{lab}	E_0^{lab} (MeV)	E_0^{inv} (MeV)	Reference
$^{27}\text{Al}(^{16}\text{O},\pi^0)X$	94	45°–75°	35±5	27±3	Present work
$^{27}\text{Al}(^{16}\text{O},\pi^0)X$	94	75°–105°	29±5	24±3	Present work
$^{27}\text{Al}(^{16}\text{O},\pi^0)X$	94	105°–135°	25±5	20±3	Present work
$^{27}\text{Al}(^{16}\text{O},\pi^0)X$	94	135°–165°	18±3	14±2	Present work
$^{27}\text{Al}(^{16}\text{O},\pi^\pm)X$	94	90°	21.7±2.4		[15]

served, similar to other cases at the same incident energy [8]. A comparison with data taken on charged pions on the same system at the same bombarding energy [15] shows that the slopes are here larger than those obtained for charged pions. However, a definite conclusion on this discrepancy cannot be drawn at this stage, since the errors are relatively large. These errors arise mainly from the limited π^0 kinetic energy range probed in this experiment because of the low statistics, since these values are extracted by the exponential tail of the spectra.

A moving source analysis has been carried out for charged pions to get the value of the temperature parameter τ and the source velocity in the framework of a thermal picture [3]. Such analysis was also performed for the present data by the momentum distribution in the source system, which is given (in the relativistic Maxwell-Boltzmann approximation) by

$$\frac{d^2\sigma}{p'^2 dp' d\Omega'} = \frac{\sigma_0}{4\pi m^3} \times \frac{e^{-E'/\tau}}{2(\tau/m)^2 K_1(m/\tau) + (\tau/m) K_0(m/\tau)}, \quad (5)$$

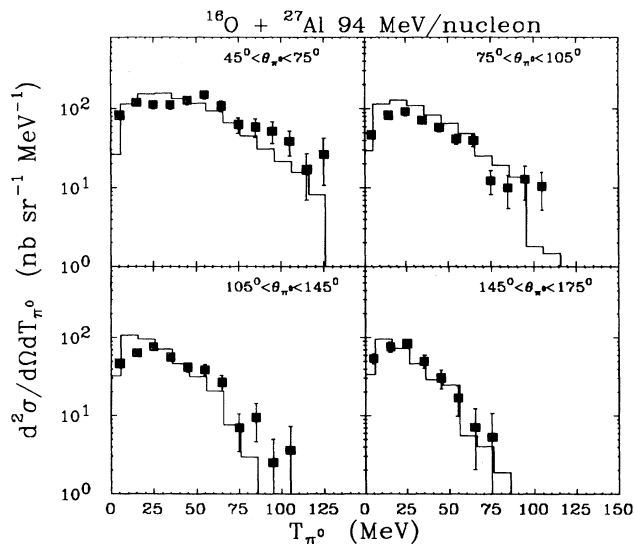


FIG. 4. Kinetic energy spectra of neutral pions in the laboratory system for several angular regions, compared to the result of a dynamical model calculation, based on the solution of the Boltzmann-Nordheim-Vlasov equation (solid histograms).

where p' and E' are the momentum and total energy, respectively, of the emitted pions of mass m , K_0 and K_1 are the modified Bessel functions of order 0 and 1, respectively, and σ_0 is the cross section for the formation of the source at a temperature τ . Transforming to the laboratory system, the differential cross section is given by

$$\frac{d^2\sigma}{d\Omega dT_{\pi^0}} = pE' \frac{d^2\sigma}{p'^2 dp' d\Omega'}, \quad (6)$$

with

$$E' = \gamma(E - \beta_0 p \cos\theta) \quad (7)$$

and

$$\gamma = (1 - \beta_0^2)^{-1/2}, \quad (8)$$

where E , p , and θ are the total energy, the linear momentum, and detection angle of the emitted pions in the laboratory system, respectively, and $v = \beta_0 c$ is the source velocity in the same system.

A simultaneous fit of the energy spectra at all angles through Eq. (6) gives a temperature parameter $\tau = 22.1 \pm 0.4$ MeV and a source velocity $\beta_0 = 0.26 \pm 0.02$. This value is consistent with a temperature of 21 ± 1 MeV reported in Ref. [8]. However, it must be stressed that both in Ref. [8] and in the present work the angular bins used to build the energy spectra are too wide, because of statistics, to allow for a good estimation of the above-mentioned parameters.

The total cross section for the production of neutral pions, evaluated by extrapolating to zero the differential cross section, was estimated to be $150 \mu\text{b}$. While the statistical error is very low (around 3%), the error arising from the overall procedure was estimated to be of the order of 30%, which also includes absolute uncertainty due to flux and target thickness. This value is in good agreement with the systematics on the integrated pion production cross section reported by several authors [6] and with the value of $175 \pm 35 \mu\text{b}$ reported in Ref. [8].

IV. DYNAMICAL CALCULATIONS

A dynamical calculation of the collision process was performed by numerically solving the Boltzmann-Nordheim-Vlasov (BNV) equation [21] with the aim of studying the emission of neutral pions, within the same approach used for the emission of energetic protons and charged pions from the same system at the same energy [15]. It is known that subthreshold pion production is

characterized by a low cross section as compared to the proton yield. For this reason the pion yield was evaluated by using a perturbative approach [22]. Each individual nucleon-nucleon collision gives a contribution to the cross section for pion production through its probability of producing a pion with a given kinetic energy and emission angle. This gives better statistics for the events of interest, which would be otherwise unattainable in the conventional approach. The BNV equation was numerically solved by means of the test particle method [21], i.e., by expressing the phase space as a collection of $N(A_1 + A_2)$ test particles, where A_1 and A_2 are the mass numbers of the colliding nuclei and N is the number of test particles per nucleon. A Skyrme mean field giving $K=200$ MeV compressibility was used to solve the Hamiltonian equation of motion and follow the time evolution of the test particles. Momentum changes of the test particles were allowed during the time evolution due to individual $N-N$ collisions. The collision integral in the BNV equation was simulated by using the concept of mean free path [22,23].

Each test particle was represented by a Gaussian to get a smooth distribution function in the phase space. At the starting time, the test particles were randomly chosen in two shifted Fermi spheres in momentum space. The number of test particles per nucleon employed in the present calculation was about 100. The pion yield was obtained from the final phase-space distribution by integrating over the impact parameter b , with step $\Delta b = 1$ fm. Calculations were performed with the same sets of parameters for all the detection angles, which were also employed for the calculation carried out for protons and charged pions for the same system at the same energy [15]. All the cuts and experimental effects were also introduced in the calculations wherever required. The elementary cross sections for pion production were taken from the parametrization of Ver West and Arndt [24].

It is known that, neglecting the pion reabsorption ($\lambda_\pi = \infty$), the calculations overestimate the experimental spectra. Pion reabsorption is frequently taken into account in a semiempirical way by introducing the attenuation factor $P = \exp(-R/\lambda_\pi)$, where R is the average path which a pion has to traverse to escape from the nuclear matter and λ_π denotes the average pion mean free path. Mean free paths ranging from 3 to 6 fm have been used in the past to reproduce absolute cross sections. In the calculation reported here, the same value of 6 fm found for charged pions [15] was used to scale also the

calculations for neutral pions. The average distance traversed by the pion was estimated by the parametrization reported in Ref. [25]. Calculated pion spectra with the above-mentioned procedure are reported in Fig. 4 as solid histograms.

As it can be seen from Fig. 4, a good agreement within the statistical errors is found with the BNV calculation in both shape and absolute value, similar to that observed for protons and charged pions [15]. It should be stressed that this agreement was obtained without any normalization of the absolute cross sections by employing the same value for the mean free path already used for charged pions.

V. CONCLUSIONS

Neutral pion production in the reaction $^{16}\text{O}+^{27}\text{Al}$ was investigated at 94 MeV/nucleon by the MEDEA BaF₂ array. Pions were clearly identified by their invariant mass. A relatively high detection efficiency was found, thus providing a good trigger for exclusive measurements.

The temperature parameter extracted by a moving source analysis was found to be consistent with that extracted from an experiment on neutral pions carried out with lead glass detectors and larger than that obtained for charged pions. The integrated cross section was found to be in agreement with the existing systematics.

Finally, the shape and absolute values of the differential cross section, such as energy spectra and angular distributions, are well reproduced by a microscopic approach based on the solution of the BNV equation, which was shown to give a good prediction also for high-energy proton and charged pion production on the same system at the same energy [15]. This shows that a consistent description of energetic products, such as high transverse momentum protons and both charged and neutral pions, can be provided in the framework of dynamical models.

ACKNOWLEDGMENTS

The authors would like to acknowledge the assistance of A. Di Stefano, F. Librizzi, M. Salemi, and A. Trovato for their technical help before and during the run. Also, the technical staff of the GANIL facility is gratefully acknowledged.

[1] P. Braun-Munzinger and J. Stackel, *Annu. Rev. Nucl. Part. Sci.* **37**, 97 (1987), and references therein.
 [2] R. Barbera *et al.*, *Nucl. Phys.* **A519**, 231c (1990).
 [3] R. Barbera *et al.*, *Nucl. Phys.* **A518**, 767 (1990).
 [4] H. Noll *et al.*, *Phys. Rev. Lett.* **52**, 1284 (1984).
 [5] H. Heckwolf *et al.*, *Z. Phys. A* **315**, 243 (1984).
 [6] J. Stackel *et al.*, *Phys. Rev. C* **33**, 1420 (1986).
 [7] E. Grosse, *Nucl. Phys.* **A447**, 611c (1985).
 [8] C. Moisan *et al.*, *Nucl. Phys.* **A537**, 667 (1992).
 [9] H. Nifenecker and J. A. Pinston, *Prog. Part. Nucl. Phys.*

23, 271 (1989).
 [10] R. Novotny *et al.*, *Nucl. Instrum. Methods A* **262**, 340 (1987).
 [11] C. Agodi *et al.*, *Nucl. Instrum. Methods A* **269**, 595 (1988).
 [12] E. Migneco *et al.*, *Nucl. Instrum. Methods A* **314**, 31 (1992).
 [13] R. Merrouch *et al.*, *Nouv. GANIL* **38**, 4 (1991); GSI Report No. 91-21, 1991.
 [14] A. Badalà *et al.*, *Z. Phys. A* (to be published).

- [15] A. Badalà *et al.*, *Phys. Rev. C* **43**, 190 (1991).
- [16] T. Matulewicz *et al.*, *Nucl. Instrum. Methods A* **289**, 194 (1990).
- [17] R. Brun, F. Bruyant, M. Maire, A. C. McPherson, and P. Zancarini, Report No. CERN-DD/EE/84-1, 1986.
- [18] A. Badalà *et al.*, *Nucl. Instrum. Methods A* **306**, 283 (1991).
- [19] H. W. Baer *et al.*, *Nucl. Instrum. Methods* **180**, 445 (1981).
- [20] C. Michel, E. Grosse, H. Noll, H. Dabrowski, H. Heckwolf, O. Klepper, W. F. J. Muller, H. Stelzer, C. Brendel, and W. Rosch, *Nucl. Instrum. Methods A* **243**, 395 (1986).
- [21] G. F. Bertsch and S. Das Gupta, *Phys. Rep.* **160**, 190 (1988).
- [22] A. Bonasera, G. Russo, and H. H. Wolter, *Phys. Lett. B* **246**, 337 (1990).
- [23] A. Bonasera, G. F. Burgio, and M. Di Toro, *Phys. Lett. B* **221**, 233 (1989).
- [24] B. J. Ver West and R. A. Arndt, *Phys. Rev. C* **25**, 1979 (1982).
- [25] W. Cassing, *Z. Phys. A* **329**, 487 (1988).